

Study of  $^{10}\text{B}(n,\alpha)^7\text{Li}$ ,  $^7\text{Li}^*$  for  $30 < E_n \text{ keV} < 500^*$ 

R. L. MACKLIN AND J. H. GIBBONS

*Oak Ridge National Laboratory, Oak Ridge, Tennessee*

(Received 28 August 1967)

We measured the cross section for  $^{10}\text{B}(n,\alpha)^7\text{Li}$  by reciprocity from the inverse reaction, using the  $4\pi$  "graphite sphere" neutron detector. The branching ratio to the ground and first excited states of  $^7\text{Li}$  was measured using face-to-face surface-barrier silicon detectors. The resulting reaction yield, normalized ultimately to the thermal cross section, shows significant ( $\geq 2\%$ ) departure from  $1/v$  in different directions at different energies for the two reaction channels:  $\geq 30$  keV (high) for  $(n,\alpha_0)$ ,  $\geq 100$  keV (low) for  $(n,\alpha_1)$ , and  $\geq 170$  keV (low) for  $(n,\alpha_0+\alpha_1)$ .

## I. INTRODUCTION

THE boron reaction has long been used as a neutron detector, flux monitor, and sometimes as a flux standard. This is because a prompt  $\gamma$  ray (478 keV) is associated with the dominant decay branch. The reaction cross section(s) have been measured in the keV range directly by Bichsel and Bonner,<sup>1</sup> Davis, Gabbard, Bonner and Bass,<sup>2</sup> and Cox<sup>3</sup> and indirectly through the total cross section by Bilpuch, Weston, and Newson<sup>4</sup>; Mooring, Monahan, and Huddleston<sup>5</sup>; and Diment.<sup>6</sup> In addition, Bergman, Isakov, Popov, and Shapiro<sup>7</sup> have measured the ratios of the absorption cross section of  $^6\text{Li}(n,\alpha)$  and  $^{10}\text{B}(n,\alpha)$  up to 30 keV, and Macklin and Gibbons<sup>8</sup> have reported values for the ground-state branch obtained from the inverse reaction.

Several authors have published values for the branching ratio. The ratio for thermal neutrons has been well determined, but values in the keV range for the partial cross section(s) and branching ratio are generally no more accurate than 10%.

The increasing importance of an accurate neutron cross-section standard for flux measurements in the energy range  $E \lesssim 500$  keV has led us to reexamine this problem. The most likely candidates for flux standards are  $\text{H}(n,p)$ ,  $^6\text{Li}(n,\alpha)$ ,  $^{10}\text{B}(n,\alpha_1\gamma)$ , and  $^{235}\text{U}(n,f)$ . Available neutron fluxes are such that it is important to have a relatively efficient detector. For most applications the detector must also be capable of fast (several nsec) timing, good discrimination against backgrounds, and

excellent stability. Proton recoil detectors become very difficult to use below 100 keV because the recoil spectrum extends to zero pulse height. Thus pulse-height discrimination against small pulses from  $\gamma$  rays, adequate at high energy, becomes nearly impossible in most experimental situations. Lithium loaded glass scintillators using the  $^6\text{Li}(n,\alpha)$  reaction have enjoyed some success but have two drawbacks. The sensitivity to  $\gamma$  rays is relatively high, leading to such complications as subtraction of the  $\gamma$  response using a  $^7\text{Li}$  loaded glass scintillator. Secondly, at the higher neutron energies, the high ratio of scattering to capture cross section smears out the time response by multiple scattering unless efficiency is sacrificed by thinning the detector. This is particularly serious as the efficiency is already low compared to  $^{10}\text{B}(n,\alpha_1\gamma)$  detectors because the lithium concentration in the glass must be held below about 5% in order not to quench the scintillator. Uranium fission counters are not efficient because the uranium layer must be thin enough to pass fission fragments. Furthermore, the resonance structure in the cross section causes difficulties if one attempts to use it in the low keV or eV range. The boron reaction does not suffer from most of these difficulties. The cross section is large [five times larger than  $^6\text{Li}(n,\alpha)$ ] and changes very slowly with energy. The reaction  $^{10}\text{B}(n,\alpha_1\gamma)$  produces a single 478-keV  $\gamma$  that enables use of a relatively high-areal-density target. The available time resolution is a few nsec. Thus we concluded that the best over-all potential cross-section standard for neutron fluxes in the energy range less than a few hundred keV is  $^{10}\text{B}(n,\alpha_1\gamma)$  and decided to improve the accuracy of the cross sections.

Our approach was to measure the inverse reaction, using the graphite sphere  $4\pi$  detector for neutrons,<sup>9</sup> which has an efficiency that is essentially independent (to  $\pm 0.3\%$ ) of energy in the range  $20 < E_n \text{ keV} < 1100$ . The only reaction branch that is available via the inverse reaction corresponds, of course, to  $^{10}\text{B}(n,\alpha_0)^7\text{Li}$ , so we had to also measure the branching ratio  $(n,\alpha_0)/(n,\alpha_1\gamma)$ . The transformation from  $\sigma(n,\alpha)$  to  $\sigma(n,\alpha_1\gamma)$  was

\* Research sponsored by the U. S. Atomic Energy Commission under contract with the Union Carbide Corporation.

<sup>1</sup> H. Bichsel and T. W. Bonner, *Phys. Rev.* **108**, 1025 (1957).

<sup>2</sup> E. A. Davis, F. Gabbard, T. W. Bonner, and R. Bass, *Nucl. Phys.* **27**, 448 (1961).

<sup>3</sup> S. A. Cox, in Conference on Neutron Cross Section Technology, Washington, D. C., 1966, edited by P. B. Hemmig, p. 701 (unpublished).

<sup>4</sup> E. G. Bilpuch, L. W. Weston, and H. W. Newson, *Ann. Phys. (N. Y.)* **10**, 455 (1960).

<sup>5</sup> F. P. Mooring, J. E. Monahan, and C. M. Huddleston, *Nucl. Phys.* **82**, 16 (1966).

<sup>6</sup> K. M. Diment, Atomic Energy Research Establishment Report No. AERE-R 5224, 1967 (unpublished).

<sup>7</sup> A. A. Bergman, A. I. Isakov, Yu. P. Popov, and F. L. Shapiro, *Zh. Eksperim. i Teor. Fiz.* **33**, 9 (1957) [English transl.: *Soviet Phys.—JETP* **6**, 6 (1958)].

<sup>8</sup> R. L. Macklin and J. H. Gibbons, *Phys. Rev.* **140**, B324 (1965).

<sup>9</sup> R. L. Macklin, *Nucl. Phys.* **1**, 335 (1957).

made on the assumption of reciprocity, viz.,

$$\frac{\sigma(\alpha, n)}{g_{\alpha n} \lambda_{\alpha}^2} = \frac{\sigma(n, \alpha)}{g_{n\alpha} \lambda_n^2}, \quad (1)$$

where  $g = (2J+1)/(2I+1)(2s+1)$ , and  $\lambda^2$  is the square of the particle-deBroglie wave length (divided by  $2\pi$ ). The energy equivalents were derived as follows. The energy available in the center of mass in the  $(\alpha, n)$  reaction is  $E(\text{cm}) \cong (7/11)(E_{\alpha} - E_{\text{threshold}})$ . In the inverse reaction, the lab neutron energy in terms of the center-of-mass energy is  $E_n(\text{lab}) \cong (11/10)E(\text{cm})$ . Thus, the lab neutron energy corresponding to the inverse reaction at  $E_{\alpha}$  is

$$E_n(\text{lab}) \cong (7/10)(E_{\alpha} - E_{\text{threshold}}). \quad (2)$$

## II. EXPERIMENTAL

### A. ${}^7\text{Li}(\alpha, n){}^{10}\text{B}$

Thin, metallic lithium targets were vacuum evaporated onto tungsten backings and transferred in an argon atmosphere to the vacuum system of the ORNL 5 mV Van de Graaff. Target thicknesses ranged from 7 to 20 keV for four MeV  $\alpha$ 's, corresponding to a neutron energy spread of 5–15 keV in the inverse reaction. Both singly and doubly charged  $\alpha$ 's were used in the measurements. The target was placed at the center of the  $4\pi$  graphite sphere neutron detector. Background was measured using the tungsten blank before the lithium evaporation. In addition, after the lithium measurement was completed the lithium was washed off with alcohol and the background was redetermined. It was equal to the preevaporation background. The background correction for energies corresponding to  $E_n \geq 30$

TABLE I. The  ${}^{10}\text{B}(n, \alpha_0)$  ground-state cross sections as calculated by reciprocity (Eqs. 1 and 2) from the  ${}^7\text{Li}(\alpha, n)$  thin-target-yield data. The cross-section scale has been normalized at 30 keV as indicated, and the  ${}^7\text{Li}(\alpha, n)$  yield data also tabulated with the same normalization. The  ${}^{10}\text{B}(n, \alpha_0)$  results are included in Fig. 1.

$\bar{E}_n^a$ keV	$\sigma(n, \alpha_0)$ b	$\bar{E}_{\alpha}$ keV	$\sigma(\alpha, n)$ mb
30	$0.2275 \pm 0.0017^b$	4425	$2.776 \pm 0.021$
41	$0.1966 \pm 0.0025$	4441	$3.267 \pm 0.042$
51	$0.1798 \pm 0.0022$	4455	$3.705 \pm 0.045$
61	$0.1632 \pm 0.0020$	4469	$4.010 \pm 0.049$
74	$0.1511 \pm 0.0018$	4488	$4.485 \pm 0.053$
90	$0.1420 \pm 0.0017$	4511	$5.10 \pm 0.06$
109	$0.1351 \pm 0.0030$	4538	$5.84 \pm 0.13$
130	$0.1290 \pm 0.0014$	4568	$6.61 \pm 0.07$
169	$0.1275 \pm 0.0024$	4623	$8.39 \pm 0.16$
190	$0.1266 \pm 0.0023$	4653	$9.31 \pm 0.17$
209	$0.1249 \pm 0.0022$	4681	$10.04 \pm 0.18$
250	$0.1246 \pm 0.0010$	4739	$11.83 \pm 0.09$
310	$0.1200 \pm 0.0009$	4825	$13.88 \pm 0.10$
371	$0.1209 \pm 0.0008$	4912	$16.44 \pm 0.11$
433	$0.1413 \pm 0.0011$	5001	$22.02 \pm 0.17$
516	$0.1566 \pm 0.0007$	5119	$28.41 \pm 0.13$

<sup>a</sup> Mean energies in three runs using thin Li metal targets of FWHM 10, 14, and 15 keV  $E_n$  equivalent. The resolution function was determined from data points below 25 keV.  
<sup>b</sup> From  $[611/(1000E_n)^{1/2}] \times (0.0689 \pm 0.0006)/1.0689$  using measured ratio near 30 keV of Table II.

keV in the inverse reaction was  $\lesssim 10\%$ .  $\alpha$  energy was calibrated by measuring the  ${}^7\text{Li}(\alpha, n)$  reaction threshold (4382 keV) and also checked at the  ${}^{19}\text{F}(\alpha, n)$  threshold (2370 keV). The uncertainty in absolute  $\alpha$ -particle energy due to energy calibration was estimated to be  $\pm 2$  keV, and the uncertainty in average neutron energy due to target-thickness effects was about  $\pm 3$  keV for thin target runs and  $\pm 5$  keV for thick (20-keV  $\Delta E_{\alpha}$ ) target runs. After correction for beam- and time-dependent backgrounds, the neutron yield was corrected for target-thickness effects, important only near threshold, by assuming a trapezoidal resolution func-

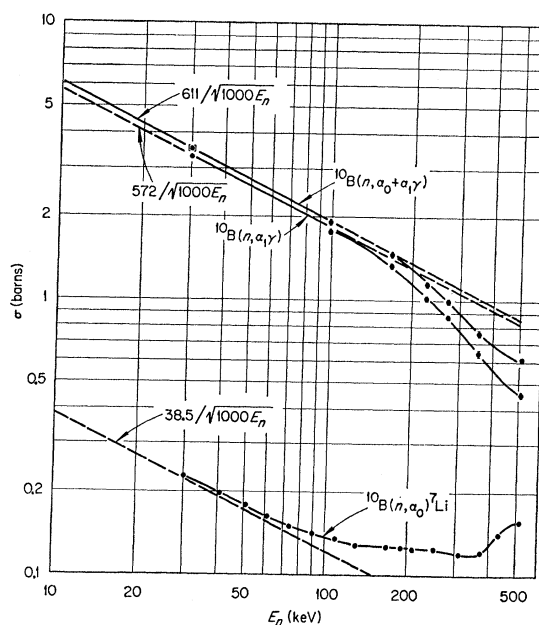


FIG. 1. The neutron-reaction cross sections of  ${}^{10}\text{B}$  from 30 to 500 keV. The lowest [ ${}^{10}\text{B}(n, \alpha_0)$ ] curve is derived by reciprocity from our thin-target  ${}^7\text{Li}(\alpha, n)$  yield data (Table I). The two upper curves are related to the lowest through our measured ratios (Table II). The cross-section scale has been normalized at the 30-keV point shown in the square bracket. Error bars are not shown where they would be too small for clarity. Error estimates for all data points are given in the tables. The total  ${}^{10}\text{B}(n, \alpha_0 + \alpha_1\gamma)$  cross section follows a strict  $E_n^{-1/2}$  dependence within 3% below 166 keV.

tion and adjusting height and width to obtain best behavior at energies closest to threshold (generally corresponding to  $E_n < 20$  keV). Best behavior was assumed to be a yield that corresponded to that expected for an infinitely thin target and inverse reaction cross section that was closely proportional to  $1/v$ . The resolution functions so obtained were in good agreement with values expected from the absolute neutron yield,  $\alpha$ -integrated current, and previously reported values of the  $\alpha, n$  cross section. They also corresponded well with our estimates of target thickness made when we prepared the target by vacuum evaporation. The target-thickness correction factor was about 15% at

$E_n=30$  keV for the thicker ( $\Delta E_\alpha=20$  keV) target and 6% for the thinner target.

The  $^7\text{Li}(\alpha, n)$  yield (neutrons per  $\alpha$ ) was measured over the full energy range for several different samples. The data were self-consistent within statistical error (usually  $\lesssim 1\%$ ). The results for a given  $\bar{E}_\alpha$  were averaged and are summarized in Table I together with the corresponding results for  $^{10}\text{B}(n, \alpha_0)$  obtained by reciprocity (see also Fig. 1). We normalized our relative cross-section measurement to an absolute cross-section scale by using the total cross-section (less scattering) results as measured by slow chopper,<sup>10</sup> crystal spectrometer,<sup>11</sup> and pulsed linear accelerator<sup>6</sup> and our own  $^{10}\text{B}(n, \alpha_0)/^{10}\text{B}(n, \alpha_1\gamma)$  ratio result (see Table II). The possible error in the relation assumed (at  $E_n=30$  keV) for the  $^{10}\text{B}(n, \alpha)$  total cross section [ $611/(1000E_n)^{1/2}$ ] has not been included in the errors estimated for each datum point.

The peak  $^{10}\text{B}(n, \alpha_0)$  cross section near 520 keV (157 mb) agrees closely with the 161 mb found by Davis *et al.*<sup>2</sup>; as they point out this is significantly lower than the 215 mb suggested by our 1959 data.<sup>12</sup> The difficulty is probably with the normalization to the  $(p, n)$  cross section we attempted at that time. Until further measurements are made, we would suggest that the cross-section scales of Figs. 12 and 13 of the 1959 paper<sup>12</sup> be reduced 25%, in line with the present normalization.

### B. Ratio Measurements

Considerable effort has been devoted to improving the precision of the  $^{10}\text{B}(n, \alpha_0)/^{10}\text{B}(n, \alpha_1\gamma)$  ratio measurements in the region where departures from the thermal neutron value become significant. In this, as in previously reported work,<sup>8</sup> we used two face-to-face surface-barrier detectors to observe the total charged particle reaction energy ( $^7\text{Li}$  recoil +  $\alpha$  particle). Use of pulsed neutrons and fast timing allowed a clean separation of the thermal neutron contribution which is particularly severe for this reaction. The thermal  $^{10}\text{B}(n, \alpha)$  cross section is about 600 times the cross section at the upper end of our energy range (500 keV).

As both  $\text{BF}_3$  and  $\text{B}_2\text{H}_6$  gas have been found to "poison" the detectors, we tried solid deposits again. They were also damaged by  $^{10}\text{B}$  evaporated directly on the detectors.<sup>13</sup>  $^{10}\text{B}_2\text{O}_3$  worked satisfactorily for a few hours, but recrystallized and dusted off very readily in the vacuum housing used during the experiment. Self-supporting  $^{10}\text{B}$  foils occasionally remained intact as long as a month and most of the measurements

TABLE II. The measured  $^{10}\text{B}(n, \alpha_0)/^{10}\text{B}(n, \alpha_1\gamma)$  ratios and the excited-state and total  $^{10}\text{B}(n, \alpha)$  cross sections<sup>a</sup> derived from the present study are tabulated. The cross sections are shown graphically in Fig. 1, and the ratios are compared with other published values in Fig. 2.

$\bar{E}_n^b$ keV	FWHM keV	Ratio	$\sigma(n, \alpha_1\gamma)^b$	$\sigma(n, \alpha_0 + \alpha_1\gamma)^b$
30	20	$0.0689 \pm 0.0006$	$[3.301 \pm 0.002]$	$[3.528]$
98	18	$0.0777 \pm 0.0016$	$1.785 \pm 0.044$	$1.925 \pm 0.045$
166	15	$0.0943 \pm 0.0010$	$1.345 \pm 0.030$	$1.473 \pm 0.032$
224	14	$0.1229 \pm 0.0019$	$1.022 \pm 0.023$	$1.149 \pm 0.025$
269	13	$0.1402 \pm 0.0022$	$0.874 \pm 0.018$	$0.995 \pm 0.019$
351	12	$0.1845 \pm 0.0043$	$0.649 \pm 0.017$	$0.768 \pm 0.018$
505	12	$0.344 \pm 0.006$	$0.458 \pm 0.009$	$0.617 \pm 0.009$

<sup>a</sup> Computed from the ground-state cross sections of Table I and Fig. 1, interpolating where necessary and propagating the errors typical of the adjacent measurements. The standard-deviation estimates shown do not include uncertainty in the  $1/v$  normalization at 30 keV, which is estimated at 0.5%.

<sup>b</sup> Uncertainty in the mean energy contributes less than 0.5% to the uncertainty of the derived cross sections at the exact energies shown.

reported here were made with an 80–100  $\mu\text{g}/\text{cm}^2$  foil of this type. We also tried thinner foils, 40–50  $\mu\text{g}/\text{cm}^2$   $^{10}\text{B}$ . These broke more quickly, but we did succeed in operating a few days with one. Unfortunately, the counter resolution and sensitivity to  $\gamma$  radiation was unsatisfactory for the higher energies during this run, and only the 30 keV point and incidental thermal data were deemed reliable. We calculated energy losses in the foils and found, for our geometry, that it was possible for  $^{10}\text{B}(n, \alpha_1)^7\text{Li}$ <sup>13</sup> occurring in a small region of a 100  $\mu\text{g}/\text{cm}^2$  foil to go undetected. If the lithium ion traversed the whole foil thickness at the maximum accepted angle, it could lose all but 100 keV or so of its energy. As the ratio measurements depended on pulses above 500 keV, this did not seem to be a problem. As a check, however, we varied the bias over a factor of 2 in one of the thick-foil runs without detecting any change in the calculated ratio as large as the few percent statistical errors.

The spectra were analyzed assuming the total resolution function for each peak was identical (above 1.5 MeV), except for a pulse-height displacement of 478 keV corresponding to the undetected  $\gamma$  ray from the excited state. The low-energy tail of the ground-state peak underlying the excited-state peak ranged from 2½% at 30 keV to 7½% at 505 keV. The small thermal neutron contributions were taken from corresponding pulse-height channels from the delayed time gate (see B, Fig. 2). The peak-area ratios were also checked with peak-height ratios. Within the poorer statistics, the latter method agreed well for the data reported. In the discarded high-energy runs mentioned earlier, this comparison showed up a spurious group a bit below the excited-state energy not due to thermal neutrons. This may have been associated with the development of damaged regions in one detector, allowing a noise pulse coincident with an  $\alpha$  particle in the other detector to be registered. Detector leakage current rose, and resolution deteriorated progressively with fast-neutron exposure.

<sup>10</sup> H. W. Schmitt, R. C. Block, and R. L. Bailey, Nucl. Phys. 17, 109 (1960); see also A. Prosdociimi and A. J. Deruytter, J. Nucl. Energy: Pt. A & B 17, 83 (1963).

<sup>11</sup> G. J. Safford, T. I. Taylor, B. M. Rustad, and W. W. Havens, Jr., Phys. Rev. 119, 1291 (1960); see also J. Als-Nielsen and O. D. Dietrich, Phys. Rev. 133, B925 (1964).

<sup>12</sup> J. H. Gibbons and R. L. Macklin, Phys. Rev. 114, 571 (1959).

<sup>13</sup> ORTEC-Model 7904 silicon surface-barrier detectors.

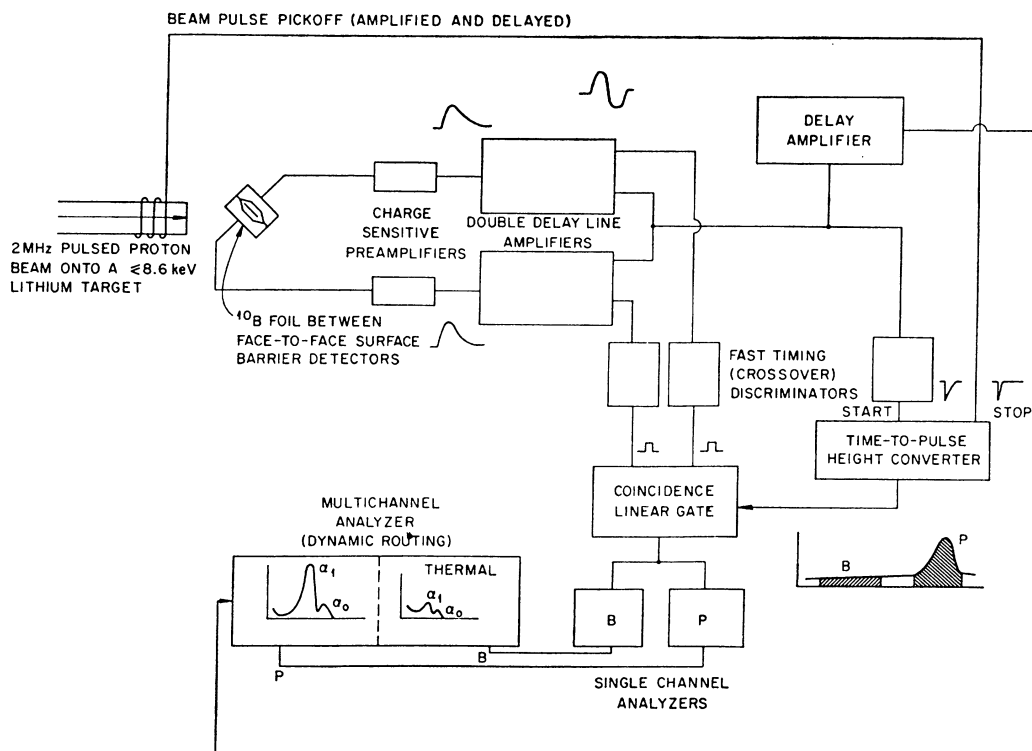


FIG. 2. Simplified block diagram for the ratio experiment. The 40 to 100  $\mu\text{g}/\text{cm}^2$   $^{10}\text{B}$  foils were mounted between two face-to-face silicon surface-barrier detectors in an evacuated thin aluminum housing (not shown). The time spectrum of neutron reactions is indicated at the lower right corner of the diagram. The time resolution was about 60 nsec and the time between neutron bursts 500 nsec. The multichannel analyzer utilized dynamic routing to record summed (coincident) pulse heights separately for the two time channels shown.

The ratio data are presented in Table II. The errors shown combine the statistical standard deviation and the effect of uncertainty in identifying the 478-keV energy difference from the spectra.

As the time gates were regularly calibrated with wax-moderated neutrons (also used for matching the gains of the two detectors), thermal ratio data were also

available from most runs. The thermal ratio result compares well with recent experiments from other laboratories as shown in Table III. Our face-to-face detector coincidence summing technique differs from the recent single detector studies<sup>14,15</sup> sufficiently to indicate the probable absence of systematic errors.

There seems to have been some confusion in the

TABLE III. The  $^{10}\text{B}(n, \alpha_0)$  ground-state yield for thermal neutrons is shown in the two usual forms; ratio to the excited-state yield, and ratio to the total  $\alpha$  yield. The values in parentheses were recalculated from the results reported for the other quantity. The results reported before 1965 lie both above and below the highly precise value of Deruytter and Pelfer<sup>a</sup> by significantly more than the errors indicated. This is also true of many less precise results from the 1950-1960 decade.

Date	Reference	$\alpha_0/\alpha_{1\gamma}$	$100\alpha_0/(\alpha_0+\alpha_{1\gamma})$	Method
1960	Brinkman & Greber <sup>b</sup>	$(0.0696 \pm 0.0005)$	$6.51 \pm 0.05$	$\text{BF}_3$ proportional
1963	Malmskog <sup>c</sup>	$0.0647 \pm 0.0007$	$(6.08 \pm 0.07)$	$\text{BF}_3$ proportional
1965	Macklin and Gibbons <sup>d</sup>	$0.067 \pm 0.002$	$(6.3 \pm 0.2)$	$^{10}\text{B}_2\text{H}_6$ semiconductors face-to-face pair
1965	Toney & Waltner <sup>e</sup>	$(0.0687 \pm 0.0012)$	$6.43 \pm 0.11$	$^{10}\text{B}$ , semiconductor
1967	Deruytter & Pelfer <sup>a</sup>	$0.06733 \pm 0.00006$	$6.308 \pm 0.006$	$^{10}\text{B}$ , semiconductor
1967	this investigation	$0.0675 \pm 0.0003$	$6.32 \pm 0.03$	$^{10}\text{B}$ , semiconductors face-to-face pair

<sup>a</sup> See Refs. 15.

<sup>b</sup> See H. F. Brinkman and D. Greber, *Kernenergie* 3, 309 (1960).

<sup>c</sup> See S. Malmskog, *Physica* 29, 987 (1963).

<sup>d</sup> See Ref. 8.

<sup>e</sup> See Ref. 14.

<sup>14</sup> W. M. Toney and A. W. Waltner, *Nucl. Phys.* 80, 237 (1966).

<sup>15</sup> A. J. Deruytter and P. Pelfer, *J. Nucl. Energy: Pt. A & B* 21, 833 (1967).

literature between the ratios

$$\sigma(n, \alpha_0)/\sigma(n, \alpha_1\gamma) = \alpha_0/\alpha_1\gamma = \alpha_0/\alpha_1 \quad (3)$$

and

$$N_\alpha/(N_\alpha^* + N_\alpha) = \alpha_0/(\alpha_0 + \alpha_1\gamma) = \alpha_0/(\alpha_0 + \alpha_1). \quad (4)$$

As these differ by nearly 7%, which of the two quantities is being reported becomes significant compared with the precision of the recent results. In Table III, we have listed both ratios. Values listed in parentheses were calculated from the quantity reported in a given reference. We have taken the expression "probability of the reaction going to the ground state of  $^7\text{Li}$ " and equivalents as indicating that (4) is being reported. In this, we rely on the standard unitary sum of probabilities. In this case, the sum of ground-state and excited-state ( $n, \alpha$ ) reaction probabilities should be one (or 100%). The term "branching ratio" customarily refers to (4) also, but fortunately in the pertinent reference<sup>14</sup> the algebraic definition is also given. "Branching ratio" is also used in a much broader sense to refer to either (3) or (4) or even<sup>5</sup> the reciprocal of (3),  $\sigma(n, \alpha_1\gamma)/\sigma(n, \alpha_0)$ .

The ratio data for 30–505 keV are compared with earlier published results in Fig. 3. The precision of the older results is comparable to the differences observed. The recent data of Sowerby appear higher than the present results above 140 keV. That author concludes however<sup>16</sup> that his reported values above 130 keV "may be in error because the wall effect of the counter may alter appreciably with energy." His reported values of  $\alpha_0/(\alpha_0 + \alpha_1\gamma)$  have been recomputed to yield the values of  $\alpha_0/\alpha_1\gamma$  plotted in Fig. 3.

### C. Excited-State and Total $^{10}\text{B}(n, \alpha)$ Cross Sections

By dividing the ground-state cross sections of Table I and Fig. 1 by the ratio data of Table II, we arrive at values for the  $^{10}\text{B}(n, \alpha_1\gamma)$  cross section. The propagated errors include the error estimates for each ratio measurement and for the ground-state cross-section measurements at adjacent energies. The total  $^{10}\text{B}(n, \alpha)$  values (Table II and Fig. 1) are simply the sum of the ground- and excited-state cross sections but their interdependence has been taken into account in calculating the error estimates.

The data are consistent with a departure of less than 3% from  $1/v$  behavior for the total  $^{10}\text{B}(n, \alpha)$  cross section below 166 keV. The ground-state cross section, on the other hand, already exceeds the low-energy (thermal)  $1/v$  dependence by 2% at 30 keV and by 32% at 166 keV. The (much larger) excited-state cross section falls significantly below the low-energy  $1/v$  extrapolation above about 100 keV. The curves shown (Fig. 1) indicate the experimental departures from  $1/v$  dependence at the higher energies. The interpolations were drawn with some guidance from detailed resonance-

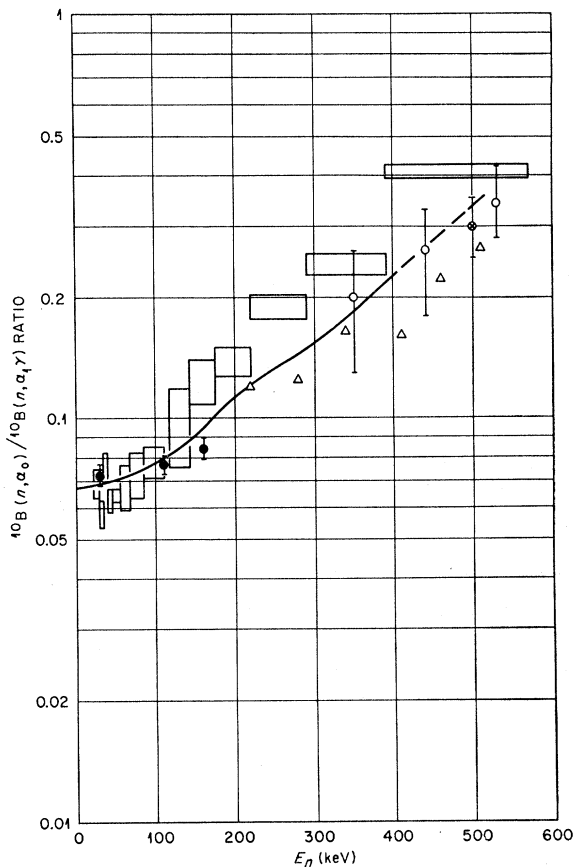


FIG. 3. Energy dependence of the ground state to excited state ratio in the  $^{10}\text{B}(n, \alpha)$  reaction from 20 to 600 keV. The results of the present experiments (indicated by the line) are in fair agreement with those of others. Dots are from our earlier work (Ref. 8) the cross from Bichsel, Halg, Huber, and Stebler [Phys. Rev. **81**, 456 (1951)] triangles from Davis, Gabbard, Bonner, and Bass, (Ref. 2), open circles from Petree, Johnson and Miller [Phys. Rev. **83**, 1148 (1951)] and the rectangles (indicating energy range and error bars) from Sowerby (Ref. 20).

parameter studies not yet completed. Briefly, in addition to an  $s$ -wave resonance near threshold,  $p$ -wave resonances near 200 and 500 keV are indicated by these (and earlier) data.  $^{10}\text{B}(d, p)$  angular distributions are being analyzed<sup>17</sup> for additional information on these states. It is already clear that the energy dependence of the total width of the  $s$ -wave threshold state implies a departure from  $1/v$  behavior. For this resonance to account for even half the thermal cross section, the implied drop below  $1/v$  dependence for the absorption cross section reaches nearly 1% in the range 5–10 keV. Above this energy, it is rapidly overcome by the  $p$ -wave resonance contributions.

### III. DISCUSSION

The total  $^{10}\text{B}(n, \alpha)$  cross section of Fig. 1 is compared with other reported values in Fig. 4. The data of

<sup>16</sup> M. G. Sowerby, J. Nucl. Energy Pt. A & B **20**, 135 (1966).

<sup>17</sup> K. K. Seth, J. H. Gibbons, and R. L. Macklin (unpublished).

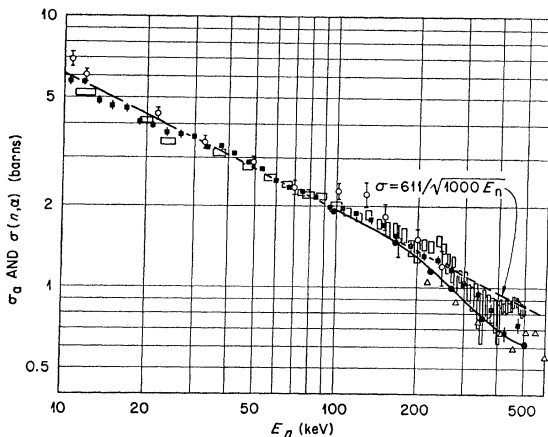


FIG. 4. Comparison of  $^{10}\text{B}$ -reaction cross sections for neutrons from 10 to 600 keV. The dots and solid line represent the present results for  $^{10}\text{B}(n,\alpha_0+\alpha_1\gamma)$ . The triangles refer to the same cross section measured relative to a modified long counter by Davis, Gabbard, Bonner and Bass (Ref. 2). The open circles represent the absorption cross section calculated from the spherical shell transmission results of Cox. (Ref. 3). The open rectangles [Mooring, Monahan and Huddleston (Ref. 5)] and the solid squares, [Diment (Ref. 6)] represent the difference between total and scattering cross sections. Differences among the several techniques are probably within the errors of measurement. Other reactions such as  $^{10}\text{B}(n,t)$  and  $^{10}\text{B}(n,\gamma)$  have been found negligible in this energy range (Ref. 5).

Mooring<sup>5</sup> and of Diment<sup>6</sup> represent the traditional method, where a neutron-scattering cross section is subtracted from the inherently highly precise neutron total cross section. The seldom-measured scattering cross section makes a major contribution above 100 keV. Earlier work from Duke<sup>4</sup> of the same general type supported a  $1/v$  dependence for  $\sigma_T - \sigma_S$  up to 70 keV "within statistical errors." The point scatter of those data appear to be about  $\pm 6\%$  (standard deviation). At still lower energies, fast chopper work has also supported  $1/v$  dependence to within several percent.

The recent shell-transmission data of Cox<sup>3</sup> represent an important independent method, but the statistical and other errors are so large that the author concludes "that the experimental results for  $^{10}\text{B}(n,\alpha)$  agree very well with the  $1/(E_n)^{1/2}$  extrapolation and with the recent results of Mooring. . ." Thus the three points between 100 and 160 keV (Fig. 4) whose error bars fall above the  $1/v$  line are not considered a significant departure.

Another traditional method is the comparison of a bare  $^{10}\text{BF}_3$  counter with a paraffin surrounded  $^{10}\text{BF}_3$  or "long counter."<sup>18</sup> The data of Davis, Gabbard, Bonner, and Bass,<sup>2</sup> shown in Fig. 3, are representative of the most careful use of this approach. Good pulse-height resolution allowed separation of thermal (and epithermal) neutron capture down to about 200 keV. Bogart<sup>19</sup>

in particular, however, has emphasized the poorly known energy dependence of the "modified long counter" efficiency below a few hundred keV. This effect apparently introduces further systematic uncertainties of many percent in the data, whose quoted error is already  $\pm 20\%$ .<sup>2</sup>

The "long counter" energy dependence has its counterpart in the present experiment where the  $4\pi$  graphite sphere detector<sup>9</sup> is relied upon for constant efficiency to  $\pm 0.3\%$ . At the 190-keV point, corresponding most closely to the back threshold in the  $^7\text{Li}(\alpha,n)$  reaction, about 3% of the neutrons have energies below 20 keV, and hence were detected with a percent or so lower efficiency. The additional correction for low graphite sphere efficiency at back threshold is thus much less than the variation of 0.3% in efficiency over the rest of the energy range covered by the inverse reaction (20–1100 keV) and quite negligible. In principle a correction could be made for the small energy dependence of the graphite sphere efficiency when the angular distributions of the  $p$ -wave resonance contributions become known.

The  $^7\text{Li}$  thin target and resolution function unfolding techniques<sup>20</sup> appear to introduce no appreciable uncertainty ( $\ll 1\%$ ) in normalizing at 30 keV or above. Below 100 keV the total-cross-section minus scattering-cross-section technique should be capable of improved precision. In two respects, one would like to rely on theory. The inverse-reaction calculation (Eqs. 1, 2) seems fundamental and for strong nuclear interactions has even been receiving some experimental support. Nevertheless, the possibility of theoretical modifications cannot be entirely dismissed. Secondly, a detailed explanation of the cross section in terms of resonance parameters should give increased confidence that significant features (such as a possible 1% drop below  $1/v$  dependence near 8 keV mentioned earlier) have not been missed, and that spurious features in the experimental data are identified.

The  $^{10}\text{B}(n,\alpha_0)/^{10}\text{B}(n,\alpha_1\gamma)$  ratio measurements in the 100–300 keV range are the most difficult part of the present approach. Neutron source strength is low; thermalized neutron effects are important and difficult to measure. Further refinement of solid-state counter techniques may help to increase the accuracy of the ratio measurements in this energy range.

#### IV. CONCLUSION

Below 166 keV, the present data, and, indeed all the reported measurements, are consistent with a  $1/v$

<sup>18</sup> A. O. Hansen and J. L. McKibben, Phys. Rev. **72**, 673 (1947).

<sup>19</sup> Donald Bogart, in Conference on Neutron Cross Section Technology, Washington, D. C., 1966, edited by P. B. Hemmig, p. 486 (unpublished).

<sup>20</sup> R. L. Macklin and J. H. Gibbons, in *Proceedings of the International Conference on the Study of Nuclear Structure with Neutrons, Antwerp, Belgium, 1965*. (North-Holland Publishing Company, Amsterdam, 1966), pp. 38, 498; Report No. EANDC-45-S, Nuclear Energy Center CEN-SCK, Belgium (unpublished).

dependence of the total  $^{10}\text{B}(n, \alpha)$  cross section to  $\pm 3\%$ . The separate ground-state and excited-state cross sections show significant departures from a  $1/v$  dependence at and above 30 and 100 keV, respectively. The measurements, extending to 505 keV, permit use of the  $^{10}\text{B}(n, \alpha)$  cross sections as a standard with a precision of a few percent even in those regions of significant departure from  $1/v$  dependence. Further high-precision measurements, preferably using several different

methods, are desirable to increase confidence in the absolute accuracy of the results.

#### ACKNOWLEDGMENTS

We are indebted to the Oak Ridge National Laboratory Target Preparation Center for the thin  $^{10}\text{B}$  foils used in the ratio measurements. Professor John L. Rodda, II (summer participant from West Virginia University), assisted in some of the data taking.

### Inadequacy of the Simple Distorted-Wave Born-Approximation Treatment of Comparative $(p, t)$ and $(p, ^3\text{He})$ Transitions\*

DONALD G. FLEMING,† JOSEPH CERNY, AND NORMAN K. GLENDENNING

*Department of Chemistry and Lawrence Radiation Laboratory, University of California, Berkeley, California*

(Received 11 September 1967)

Current theories of direct two-nucleon transfer reactions are tested, by comparing  $(p, t)$  and  $(p, ^3\text{He})$  transitions on odd-mass nuclei leading to mirror final states. Proton-induced reactions on  $^{15}\text{N}$  at 43.7 MeV and on  $^{13}\text{C}$  at 49.6 MeV are discussed in detail. Many mirror transitions are analyzed with DWBA calculations in an attempt to fit both angular distributions and cross-section ratios; good results for the shapes of the angular distributions are obtained. The agreement between theory and experiment for the cross-section ratios of mirror  $(p, t)$  to  $(p, ^3\text{He})$  transitions improves in every case with the inclusion of a strongly spin-dependent force in the nucleon-nucleon interaction, but over-all satisfactory agreement is not obtained. The  $(p, t)$  transitions are found to be generally stronger than expected, relative to their mirror  $(p, ^3\text{He})$  transitions, and three cases are discussed where the experimental ratios of these cross sections exceed the theoretical upper limit. Two possibilities, both of which introduce coherent effects, are discussed to account for this result: (1) interference terms arising through a spin-orbit interaction in the optical potential or (2) interference terms between a direct-reaction contribution and a core-excitation contribution to the cross section.

#### I. INTRODUCTION

EARLIER work has shown the utility of comparative  $(p, t)$  and  $(p, ^3\text{He})$  transitions in investigating the charge independence of nuclear forces<sup>1</sup> and in identifying states of high isospin—in particular,  $T = \frac{3}{2}$ <sup>2</sup> and  $T = 2$ <sup>3</sup> levels. In addition, however, similar comparative measurements of these reactions on odd mass ( $T = \frac{1}{2}$ ) targets populating mirror final states provides one with a sensitive test of some of the assumptions made in current theories of direct two-nucleon transfer reactions.<sup>4,5</sup>

\* Work performed under the auspices of the U. S. Atomic Energy Commission.

† Present address: Nuclear Structure Laboratory, University of Rochester, Rochester, N. Y.

<sup>1</sup> J. Cerny and R. H. Pehl, Phys. Rev. Letters **12**, 619 (1964).

<sup>2</sup> C. Detraz, J. Cerny, and R. H. Pehl, Phys. Rev. Letters **14**, 708 (1965); J. Cerny, R. H. Pehl, G. Butler, D. G. Fleming, C. Maples, and C. Detraz, Phys. Letters **20**, 35 (1966).

<sup>3</sup> J. Cerny, R. H. Pehl, and G. T. Garvey, Phys. Letters **12**, 234 (1964); G. T. Garvey, J. Cerny, and R. H. Pehl, Phys. Rev. Letters **12**, 726 (1964).

<sup>4</sup> N. K. Glendenning, Ann. Rev. Nucl. Science **13**, 191 (1963); Phys. Rev. **137**, B102 (1965).

<sup>5</sup> J. R. Rook and D. Mitra, Nucl. Phys. **51**, 96 (1964); C. L. Lin and S. Yoshida, Progr. Theoret. Phys. (Kyoto) **32**, 885 (1964); E. M. Henley and D. V. L. Yu, Phys. Rev. **133**, B1445 (1964); B. Bayman, Argonne National Laboratory Report No. ANL-6878, p. 335, 1964 (unpublished); A. Y. Abul-Magd and M. El Nadi,

Of particular interest in such  $(p, t)$  versus  $(p, ^3\text{He})$  comparisons is an understanding of the influence of the greater flexibility of the  $(p, ^3\text{He})$  reaction, which in first order permits a  $^3\text{S}$  and  $^1\text{S}$  spin-isospin transfer of a neutron-proton pair, as compared to the  $(p, t)$  reaction, which only allows a  $^3\text{S}$  transfer of two neutrons. The population of mirror final states permits such comparisons with minimal uncertainty in the final-state wave functions. In most previously reported work,<sup>1-3</sup> such comparisons were not discussed because final states of high isospin were of interest, and hence a pure  $^3\text{S}$  transfer of both nucleon pairs was required.

In general, it is found that  $(p, t)$  cross sections to mirror final states—when not inhibited by nuclear structure considerations—are strongly enhanced over the corresponding  $(p, ^3\text{He})$  transitions, sometimes by factors as large as 4 or 5, and we will consider the implications of this enhancement in some detail. The only previous work discussing  $(p, t)$  and  $(p, ^3\text{He})$  transitions to mirror final states has been by Cerny *et al.*,<sup>6</sup> who recently studied the mass 5 and mass 7 final nuclei

Nucl. Phys. **77**, 182 (1966); V. S. Mathur and J. R. Rook, *ibid.* **A91**, 305 (1967).

<sup>6</sup> J. Cerny, C. Detraz, and R. H. Pehl, Phys. Rev. **152**, 950 (1966).